Bulletin of Engineering Geology and the Environment (2026) 85:218
https://doi.org/10.1007/s10064-026-04883-6

ORIGINAL PAPER

Precise diagnosis of mixed-face ground through distributed cutter working status monitoring data in slurry TBM

Wei Xiaolong[1,2] · Wang Shuangjing[2] · Zhao Yunbo[1,3] · He Fei[2] · Dong Yue[2] · Wang Jing[4]

Received: 22 May 2025 / Accepted: 11 March 2026

Abstract

Geological data for tunnel construction is usually acquired through surface drilling. However, due to constraints such as limited borehole spacing, the obtained information may deviate from actual subsurface conditions. This can lead to inaccurate decision-making during tunnel boring machine (TBM) operation, ultimately affecting construction progress. To evaluate the ground along tunnels accurately, this paper presents a precise diagnostic method for the tunnel face based on the rotation speed of the disc cutter. First, we propose diagnosing the tunnel face on the basis of the rotation speed of the disc cutter. Second, the cutter rotational speed ratio ($\boldsymbol{R_n}$) is proposed as a parameter for assessing rock hardness. This parameter, in conjunction with the installation positions and rotation angles of all the disc cutters on the cutterhead, can describe the mixed ground conditions of the tunnel face. A case study in the Zhuhai slurry TBM tunnel indicates that the proposed method can distinguish different ground types in tunnel faces. To validate the results, the cutterhead extrusion force was introduced. The findings show that the proposed method can obtain a precise diagnosis of mixed-face ground, which can be useful for tunneling parameter operation.

Keywords Slurry TBM · Mixed-face ground · Distributed cutter monitoring data · Cutter rotation speed ratio · Precise diagnosing

Introduction

Currently, large-diameter tunneling boring machines (TBMs) are widely used in tunnel construction. Expansion of large-diameter, long-distance slurry TBM tunnels under high water pressure will increasingly encounter complex geological conditions, including mixed ground, boulder ground, and shallow overburden (Li et al. 2017; Ma et al. 2015; kos Tóth et al. 2013). Such challenging ground conditions raise considerable risks for TBM tunneling, such as TBM attitude deviation, abnormal vibration, and accelerated cutter wear. These issues lead to deviations in the tunneling direction or an increase in disc cutter change time (Farrokh 2021), as shown in Fig. 1. The tunnel face is the key location where rock–machine interactions occur. Therefore, it is highly important to accurately identify the geology in a tunnel face during TBM operation to improve safety and reduce construction costs.

During shield TBM tunnel construction, geological exploration, tunneling data analysis, indirect analysis, and direct detection methods are usually adopted for ground diagnosis.

✉ Zhao Yunbo
ybzhao@ustc.edu.cn

Wei Xiaolong
13592503035@126.com

Wang Shuangjing
874032705@qq.com

He Fei
tbm666@126.com

Dong Yue
dydyddy90@qq.com

Wang Jing
wjingsdu@163.com

1 Department of Automation, University of Science and Technology of China, Hefei, Anhui, China

2 China Railway Engineering Equipment Group Co., Ltd., Zhengzhou, Henan, China

3 Institute of Artificial Intelligence, Hefei Comprehensive National Science Center, Hefei, Anhui, China

4 School of Qilu Transportation, Shandong University, Jinan, Shandong, China

Published online: 21 March 2026

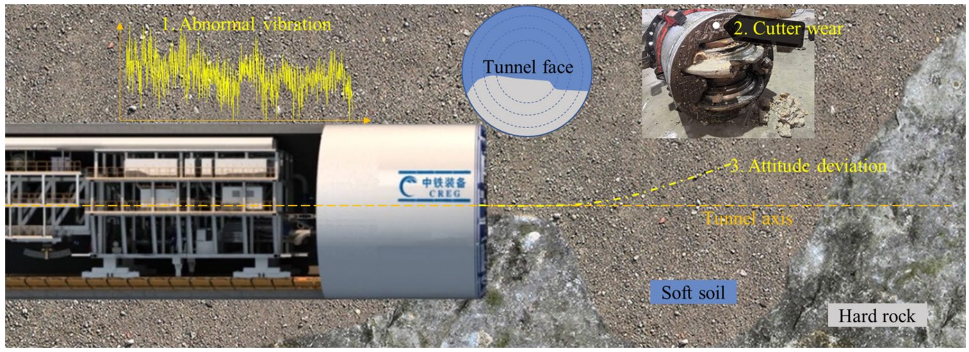

Fig. 1 Risks during TBM operation on mixed-face ground

(1) Geological exploration method: This method is typically used for early stages of project construction (Xie et al. 2023). It is a method for the preliminary interpretation of the ground conditions along the tunnel axis in combination with sparse boreholes (Zhang et al. 2023). However, limited by the cost of boreholes and difficulty in operation, this methods cannot efficiently drill dense boreholes during TBM operation (Li et al. 2020); thus, it fails to describe the geological characteristics of a tunnel precisely.

(2) Tunneling data method: TBM tunneling parameters serve as key indices reflecting the rock–machine interaction; accordingly, the geological distribution of the tunnel face can be judged on the basis of the data ranges under different ground conditions. kos Tóth et al. (2013) proposed a correlation between mixed-face ground characteristics and TBM operational parameters; Vergara et al. (A and B 2017) analyzed the characteristics of tunneling parameters in mixed-face ground and proposed the MFPI to illustrate mixed-face ground; Qi et al. (2021) proposed a model for mixed-face ground prediction using the total thrust force and torque. However, tunneling parameters such as cutterhead extrusion usually reflect the average geological characteristics of a tunnel face and fail to identify the precise features of different areas on the tunnel face.

(3) Indirect analysis method: As muck is the fragmented result of the surrounding rock at the tunnel face, its properties can be analyzed to assess the ground conditions during excavation. Gong et al. (2020) developed an intelligent muck identification system for the belt conveyor to realize the real-time measurement of muck volume and mass; Xie et al. (2023) used a muck image analysis method for the real-time detection of rock–machine interactions; Lee and Kwon et al. (G.-J. and T.-H. 2023) studied the discharge behavior of spherical and rock chip muck via screw conveyors. However, muck volume can reflect only the ratio of the hard rock area on the tunnel face but not its distribution.

(4) Direct detection method: Most methods fail to identify the precise features of different areas on the tunnel face, Entacher et al. (2012, 2013) utilized forces acting on disk cutters to diagnose the ground. In this method, an instrumented cutter was designed to monitor cutting forces, temperature and rotation of the disc cutter. However, its installation method presents challenges for large-scale engineering applications. Moreover, as the primary measured variable is force, it is easily affected by sensor noise.

In this article, we propose a direct detection method that can precisely diagnose the mixed-face ground of a tunnel face on the basis of the rotation speed of the disc cutter. To avoid reliability issues, the hardness of the face is not judged by the force exerted on the disc cutter. First, we propose a system principle for the precise diagnosis of mixed-face ground systems. Second, we propose a method for the precise diagnosis of mixed-face ground conditions based on the rotational status of distributed disc cutters. Third, the proposed method is applied to diagnose the mixed-face ground of the Zhuhai Tunnel Project. Fourth, a comparison of the results obtained via the proposed method with those obtained via exploration is followed by a comprehensive discussion. Finally, a conclusion is drawn. Compared with previous methods, the approach proposed in this paper offers the following improvements.

(1) The proposed method is suitable for the precise and continuous diagnosis of mixed geology and can identify the interface between hard and soft geological layers.

(2) The method is based on the rotation speed of the disc cutter and has high reliability.

(3) The proposed method is suitable for large-scale engineering applications.

Theoretical foundation for the diagnosis of mixed-face ground conditions

Forces acting on the disc cutter during rock breaking

Cutters are installed in the cutterhead, which is subjected to a normal force and a tangential force. Cutter rotation and rock breakage are accompanied by rotation of the cutterhead, and multiple distributed cutters can realize the full face rock breaking of the tunnel. To a certain extent, the rock breaking process of the cutter can be simplified as a linear cutting process. The schematic in Fig. 2 illustrates the forces acting during the process of rock breaking by disc cutters.

Many rock breaking models have been proposed for the linear cutting process of the cutter, among which the CSM model is among the most famous and widely used models. In the CSM model, the resultant force F_t of the cutter during the rock breaking process is shown in Eq. 1. Normal forces F_n along the vertical direction and the tangential force F_r along the horizontal direction can be obtained through the decomposition of the resultant force F_t, as shown in Fig. 2. The surrounding rock exerts a resistance force on the disc cutter. F_r' is the tangential resistance force exerted by the rock, which is equal in magnitude to F_r but acts in the opposite direction. F_n' is the normal resistance force exerted by the rock, which is equal in magnitude to F_n but acts in the opposite direction. Detailed information can be found in the literature (Rostami et al. 1996).

$$F_t = \frac{Pwr\phi}{1+\Psi} \tag{1}$$

In Eq. 1, Ψ is the constant for the pressure distribution function; w is the tip thickness or width, mm; r is the radius of the cutter, mm; ϕ is the angle of contact between the rock and disc cutter, which can be represented as Eq. 2:

$$\phi = \arccos\left(\frac{r-p}{r}\right) \tag{2}$$

P is the pressure in the crushing zone, which is related to the rock strength, cutter size, and cutter ring shape, and it can be calculated as follows: Eq. 3 (Feng 2019);

$$P = C\sqrt[3]{\frac{S}{\phi\sqrt{rw}}\sigma_c{}^2\sigma_t} \tag{3}$$

where S is the disc cutter spacing, mm; C is a dimensionless coefficient, taken as 2.12; σ_c is the uniaxial compressive strength of the rock, MPa; and σ_t is the tensile strength of the rock, MPa.

Under the action of the resultant force, the normal force F_n and the tangential force F_r can be obtained through Eq. 4 (Feng 2019).

$$\begin{cases} F_n = F_t\cos\frac{\arccos\frac{r-p}{r}}{2} \\ F_r = F_t\sin\frac{\arccos\frac{r-p}{r}}{2} \end{cases} \tag{4}$$

According to Eqs. 1, 3, 4, the tangential force F_r can be represented as follows:

$$F_r = \frac{C\sqrt[3]{\frac{S}{\arccos\frac{r-p}{p}\sqrt{rw}}\sigma_c^2\sigma_t}wr\Psi}{1+\psi}\cdot\sqrt{\frac{2p-r}{2p}} \tag{5}$$

The tangential force F_r enables the rotation of the disc cutter, which is related to rock strength, dics cutter radius and penetration. The relationship between the rotation state of the cutter and the geology are discussed below.

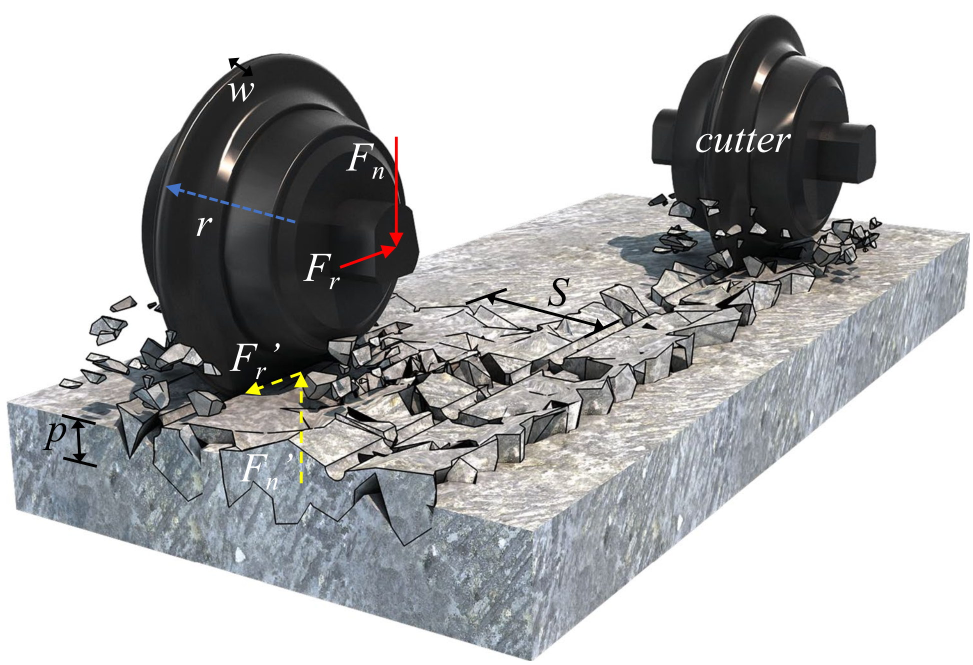

Fig. 2 Force analysis schematic for disc cutters rock-breaking process

Conditions for disc cutter rotation

The start-up torque is a certain torque to overcome the frictional force on the bearing of the cutter and surrounding rock, and it can be expressed as the product of the cutter radius and tangential force. On the basis of Eq. 5, for a given project and disc cutter,

The tangential force F_r can be expressed as a function of the penetration p and uniaxial comprehensive strength σ_c. F_r increases with increasing p when σ_c is constant, and F_r increases with σ_c when p is constant.

Taking a 17-inch disc cutter as an example, the start-up torque is approximately 40 Nm, and the cutter radius is 216 mm; thus, the cutter rotates while the tangential force is greater than 0.18 kN, which is the rotation condition for the 17-inch disc cutter. Moreover, there exists an area where F_r is less than 0.18 kN, with a smaller σ_c and p. Figure 3 shows the trend of relevant parameters for a 17-inch disc cutter as an example.

For the 17-inch disc cutter, normal rotation can be achieved when the uniaxial compressive strength σ_c of the rock mass is high, and the tangential force F_r acting on the disc cutter exceeds 0.18 kN. Conversely, under low σ_c conditions where the tangential force is less than 0.18 kN, the disc cutter would rotate normally. Tóth et al. defined mixed-face ground where the uniaxial compressive strength ratio is at or lower than 1/10 between that of the weakest and strongest rock (soil). Given the aforementioned analysis, the uniaxial compressive strength of rocks in the stratum can be discriminated by monitoring the disc cutter rotation speed, which consequently facilitates the diagnosis of mixed-face ground conditions.

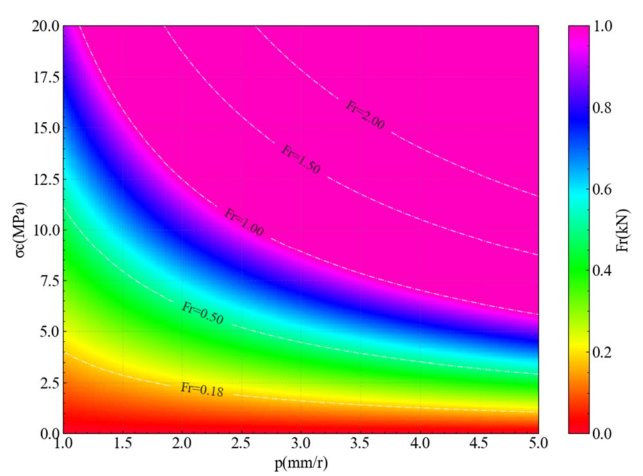

Fig. 3 Tangential force F_r for different σ_c and p. Note: Consider a conventional slurry TBM cutterhead with 17-inch disc cutter as an example, the values in Eq. 3 are: $C = 2.12$, $S = 75$mm, $r = 216$mm, $w = 20$mm, Supposing $\sigma_c = 10\sigma_t$, $\Psi = 0$

Method for the precise diagnosis of mixed-face ground

In accordance with the theoretical methodologies introduced previously, a novel method for stratum diagnosis is proposed, as shown in Fig. 4. This method contains three steps: data processing, feature extraction and tunneling facial reconstruction.

Step 1: Data processing, which focuses on effective data extraction from the multisource database of the disc cutter rotation speed n_k and cutterhead rotation speed N and cutterhead extrusion force F during the tunneling process.

Step 2: Feature extraction, which uses an index named the cutter rotation speed ratio R_n, to normalize the rotational speeds of the disc cutters n_k at different positions on the cutterhead.

Step 3: Geological analysis, which aims to acquire the full-face characteristic through distributed cutter rotation speed ratio R_n of different disc cutters.

Data processing

The TBM tunneling data reflect the TBM status, including the cutterhead rotation speed, extrusion force, torque and so on. These data can be obtained from the PLC of the TBM, and the acquisition frequency is 1 second per iteration. In addition, the disc cutter monitoring data present the disc cutter working status, including the rotation speed and temperature of the disc cutters. The acquisition frequency is affected by the working structure and the wireless communication environment, ranging from 20 to 60 seconds per iteration. To align different data sources, all data are uniformly stored on the basis of the acquisition frequency of the disc cutter working status data, 20–60 s per iteration. The stored data include the (i) ring number, (ii) cutterhead rotation speed, (iii) cutterhead extrusion force, (iv) disc cutter installation angle, and (v) disc cutter rotation speed.

The tunneling period refers to the effective tunneling period of the TBM, during which data such as the cutterhead rotation speed N and the cutterhead extrusion force F are not equal to 0. In contrast, these data remain at zero during the downtime period (Li et al. 2023). On the basis of characteristics above, the method from Wang et al. is used to preprocess the tunneling parameters (Wang et al. 2021).

$$D = \begin{cases} 0, N \cdot F = 0, \text{down time period} \\ 1, N \cdot F > 0, \text{tunneling period} \end{cases} \quad (6)$$

We select the tunneling data and the disc cutter monitoring data according to the ring number, and then we obtain the valid data by using Eq. 6 to exclude the data when the cutterhead rotation speed and the thrust force are 0.

Fig. 4 Flow chart for mixed-face ground diagnosis

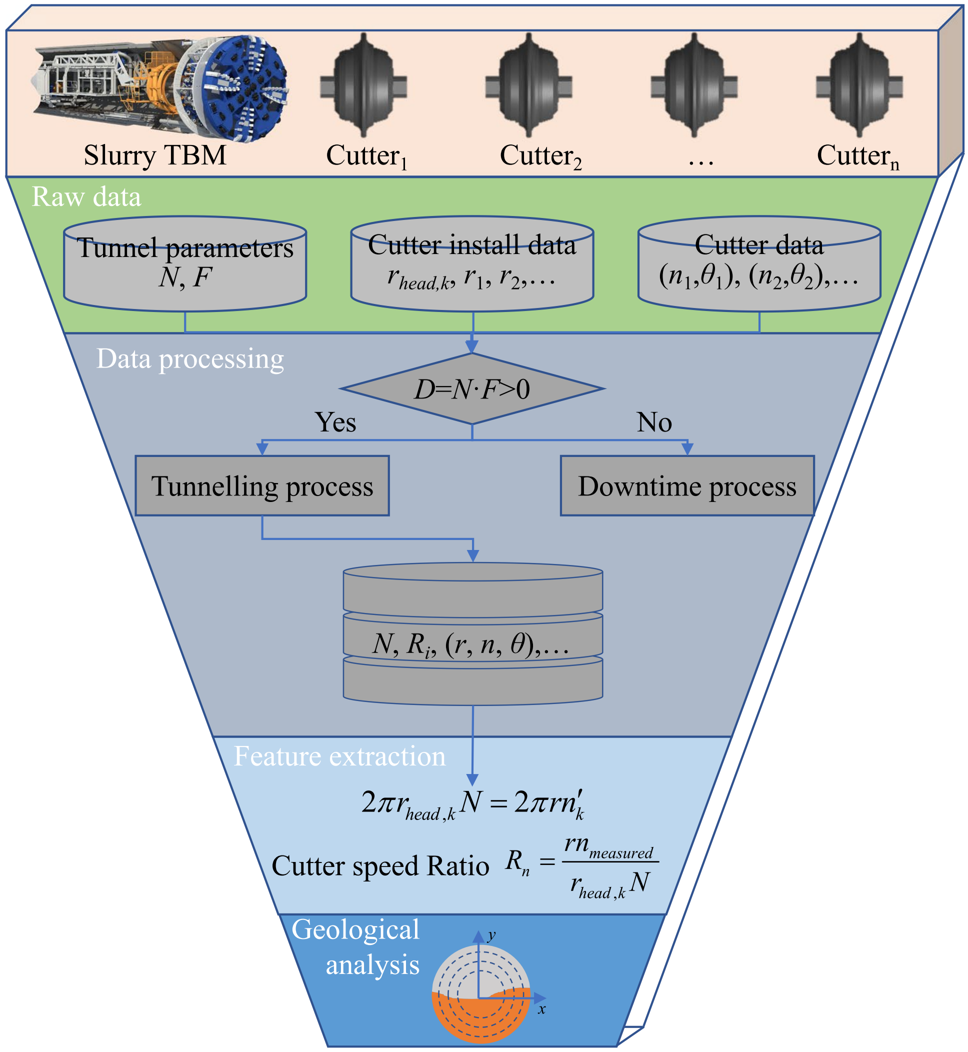

Feature extraction

Notably, to reflect the rotational speed data characteristics of the disc cutters at different spatial positions, we store the rotational speed data according to the real-time angular position of the disc cutters to ensure that they reflect the the disc cutter status at different spatial positions.

During the tunneling process, the real-time angle of the cutterhead is stored, denoted as $\theta_h = [0°, 360°]$. θ_h can be obtained from the PLC. As the cutterhead is a rigid structure, each disc cutter has a fixed angle with the zero-degree position of cutterhead, which we call the installation angle of the disc cutter, denoted as $\theta_c = [0°, 360°]$. This value can be provided by structural designers. The real-time angle of the disc cutter can be expressed as follows:

$$\theta = \theta_h + \theta_c \tag{7}$$

By monitoring the real-time rotational speed of the k-th disc cutter, named n_k, and the real-time angle of the disc cutter θ, we can obtain the distribution characteristics of the disc cutter's rotational speed data at different spatial positions. These can be plotted in polar coordinates (n_k, θ). Here, we use a 15-meter-diameter slurry TBM as an example to illustrate, and three cutters on the cutterhead, namely, 22#, 47#, and 66#. The locations of these cutters are illustrated in Fig. 5.

Figure 6 illustrates the rotational speed data for the three cutters at various spatial positions. The figures are presented in polar coordinates, with each cutter distinguished by a different color. Each point in a figure represents a set of monitoring data, with the distance from the center of the circle representing the magnitude of the rotational speed n_k, and the angle at which the point is located representing the real-time angle position of the disc cutter a.

The rotational speeds of the disc cutters at various positions differ considerably. This difference arises because the disc cutters lack independent driving mechanisms and crush rock individually. Additionally, the installation radii of each disc cutter, which refers to the distance from the

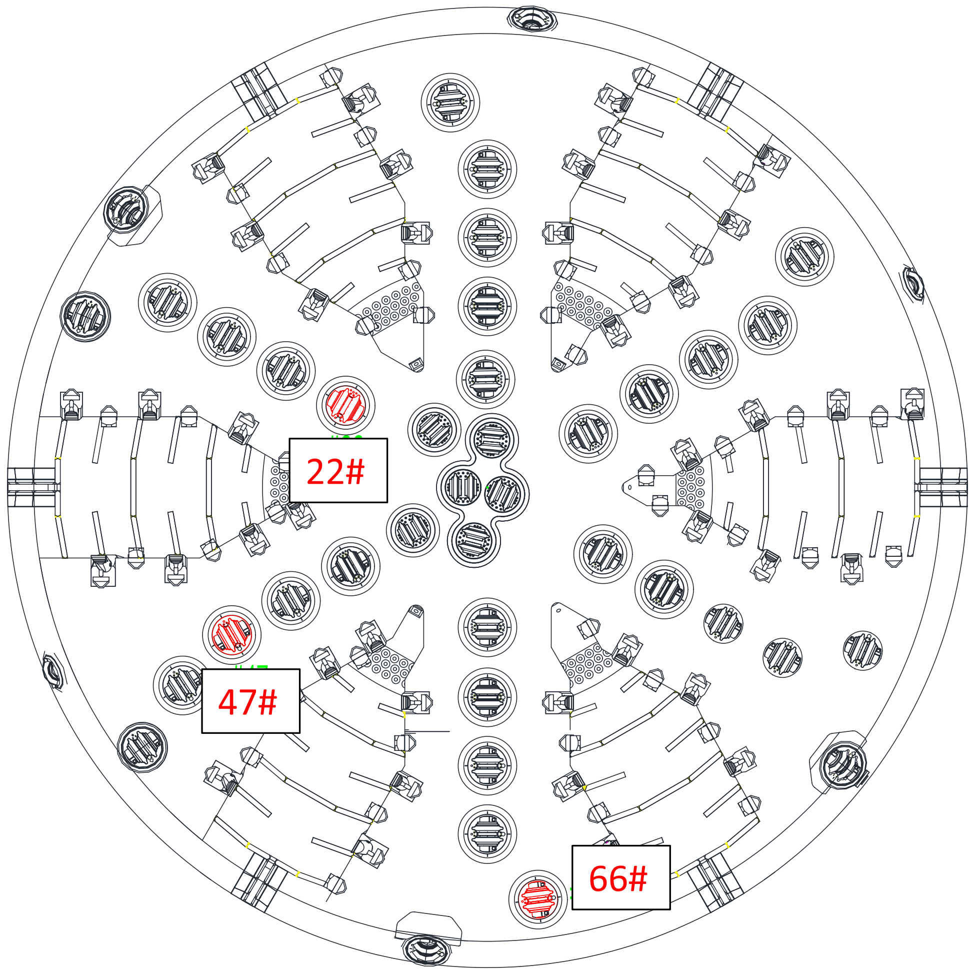

Fig. 5 Distribution of disc cutters on the cutterhead

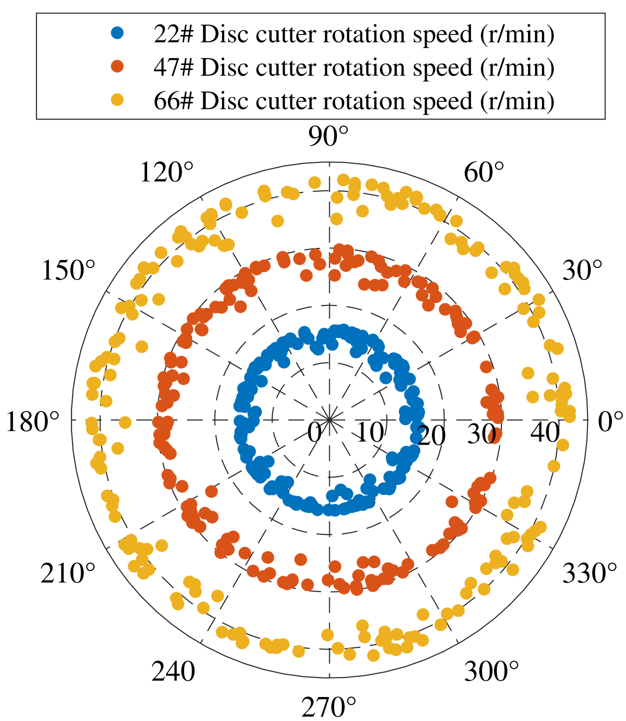

Fig. 6 Rotation speeds of three disc cutters in a single ring

disc cutter's installation point to the center of the cutter head, vary. Under identical circumferential speed of the cutter head, a larger installation radius results in a greater linear velocities and angular velocities for the disc cutter. The theoretical rotational speed of a disc cutter is a function of the cutter head speed and its position on the cutter head. For instance, on a cutter head with a 15-meter excavation diameter, the installation radius is approximately 2500 mm for the 22# disc cutter but approximately 6700 mm for the 66# disc cutter. Assuming a 19-inch cutter with a radius of 241.3 mm and a cutter head circumferential speed of 1.5 revolutions per minute, the rotational speed of the 22# disc cutter would be approximately 15 revolutions per minute and that of the 66# disc cutter would be approximately 41 revolutions per minute.

Owing to the considerable rotational speed variations across different installation radii of the disc cutters, it is challenging to accurately determine the rotational state of the disc cutter and establish a unified standard for evaluating their state on the basis of their rotational speed. For this reason, we propose a method for normalizing the rotational speed data of the disc cutters.

The theoretical linear speed of the disc cutter ring is equivalent to the linear speed at the point where the disc cutter is situated on the cutterhead, as follows:

$$2\pi r_{\text{head},k} N = 2\pi n_k' \tag{8}$$

where $r_{\text{head},k}$ is the k-th disc cutter installation radius (referring to the distance between the cutterhead center and the k-th disc cutter), in mm; N is the cutterhead rotation speed in units of of r/min; r is the radius of the disc cutter; and n' is the theoretical disc cutter rotation speed, with units of r/mim. We refer to the linear speed at that point on the cutterhead as the theoretical linear speed of the disc cutter ring.

On the basis of the previous analysis, if the geological conditions are relatively soft, the tangential force F_r acting on the cutterhead is small and fails to meet the starting condition for the disc cutter's rotation. Consequently, the disc cutter cannot rotate continuously and stably, and the actual linear speed of the disc cutter ring will be lower than the linear speed at the corresponding point on the cutterhead.

Using Eq. 8, along with the radius r of the unworn cutter, the theoretical rotational speed n of the disc cutter can be calculated. Additionally, the actual rotational speed n_k of the disc cutter can be obtained through sensor measurement. On the basis of these quantities, the index of the disc cutter rotation speed ratio R_n is proposed to normalize the disc cutter rotation status. R_n is the ratio of the actual disc cutter rotation speed to the theoretical value, as shown below:

$$R_{\text{n}} = \frac{n_k}{n_k'} \tag{9}$$

Compared with the disc cutter rotational speed n_k, R_n eliminates the influence of the disc cutter installation radius and the cutterhead speed. This method features a clear theoretical basis, straightforward calculation, and convenient implementation and applies to cutterheads of varying diameters.

If the geological conditions are relatively hard and the cutter experiences a large F_r, meeting the cutter rotation start-up condition, then R_n is always approximately 1. If the geological conditions are relatively soft and the cutter rotation is discontinuous, then $R_n < 1$ or even equals 0. There is a special case here: if the cutter's radius decreases because of wear, the linear speed of the cutter ring remains equal to the linear speed at that point on the cutterhead, but the actual speed of the cutter will exceed the theoretical speed, resulting in $R_n > 1$. However, this case has a limited influence on the results of geological analysis. The speed ratio calculation results of the data in Fig. 6 are shown in Fig. 7. The rotational speed ratio of different disc cutters is a comprehensive index that is unaffected by the cutterhead speed and installation radius. It reflects the severity of the cutter's rolling slip, thus providing a basis for determining the ground conditions.

Full-face reconstruction of tunneling ground conditions based on disc cutter rotational speed ratios

Figure 7 illustrates the distribution characteristics of the rotational speed ratio for an individual disc cutter, revealing the ground conditions within the disc cutter's specific installation radius. Next, we want to further obtain the geological distribution of the entire excavation of the face. For this purpose, a geological fine analysis method based on the state monitoring data of all discs cutters on the cutterhead is proposed.

Assuming that m disc cutters are on the cutterhead, we divide the entire circular excavation surface into m discrete circular rings on the basis of the total number of disc cutters and their respective installation radii, extending from the center to the edge. Each ring corresponds to a single cutter. Furthermore, each ring is evenly divided into 360 sector areas, with each area spanning 1 degree around the circumference. Therefore, the entire excavation face is divided into $(360 \times m)$ discrete regions. Next, the average speed ratio of the cutters in each region is calculated. This value is obtained by calculating the average of all the speed ratios

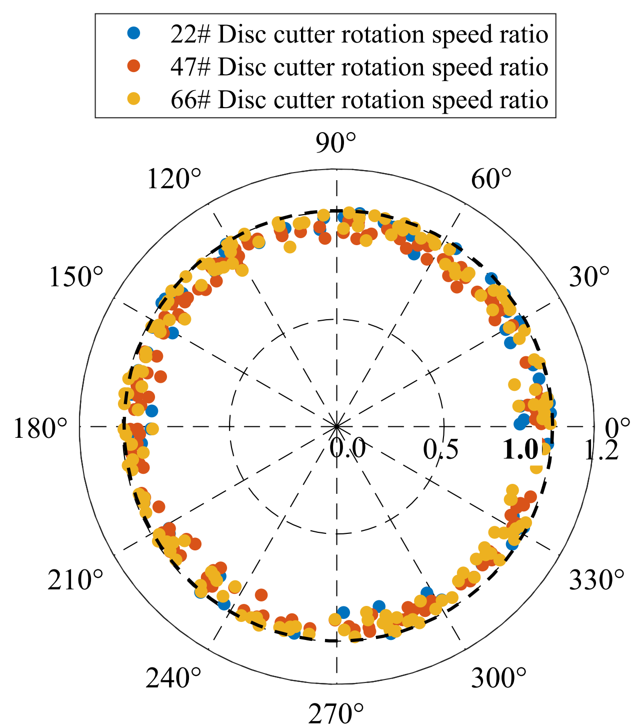

Fig. 7 Rotation speed ratios of three disc cutters in a single ring

monitored when the k-th cutter satisfies the real-time angle θ_k within the range $[i^\circ, i+1^\circ)$, which is denoted as $\overline{R_{\mathrm{n},k,i}}$. Here, k represents the disc cutter index, and i represents the rounded value of the cutter's rotation angle. Thus, we construct the expression form of $(\theta_i, r_k, \overline{R_{n,k,i}})$.

On this basis, we can construct a distribution map of the rotational characteristics of the disc cutters throughout the cutterhead area: At each point (a_i, r_k), $\overline{R_{\mathrm{n},k,i}}$ is displayed in different colors. When $\overline{R_{\mathrm{n},k,i}} = 1$, the point is green, indicating that the cutter is rotating well; when $\overline{R_{\mathrm{n},k,i}} = 0$, the point is red, indicating that the cutter is not rotating; between 0 and 1, the color transitions naturally from green to red.

Figure 8 illustrates the process of identifying the full-face tunnel face geological conditions by combining the rotational speed ratios of individual disc cutters with their positions on the cutterhead. In the upper portion of this figure, the various rings correspond to the data characteristics of different independent cutters. The lower portion of the figure illustrates the data characteristics of the complete excavation surface. Notably, in actual engineering, owing to the possibility of sensor failures, the data may be incomplete, which will result in some circular trajectories in the final analysis graph not being displayed and appearing in white.

According to the introduction in Section "Conditions for disc cutter rotation", under the same penetration, the lower the uniaxial compressive strength, the smaller the tangential force is, and the rotation state of the disc cutter is worse. Conversely, the higher the uniaxial compressive strength is, the greater the tangential force is, and the rotation state of the disc cutter is better. Therefore, utilizing this, the rotation speed ratio can effectively indicate whether the disc cutters meet the rotational torque requirements. Thus, depending on the distribution of the disc cutter rotation speed ratio, the condition of the surrounding rock can be distinguished precisely.

Precise diagnosis of mixed-face ground: a case study

Overview of the project and system

In this work, we apply the proposed method to the Zhuhai Tunnel Project. This project is located in Zhuhai city, Guangdong Province, China. It starts from the east of Zhuhai Bridge and ends at the west, with the alignment parallel to the southern side of the existing Zhuhai Bridge. The tunnel passes through the Modaomen Waterway and is constructed by the slurry TBM method. The outer diameter of the tunnel is 14.5 m, and the length of the TBM section is 2.93 km, of which approximately 2.70 km is underwater, as shown in Fig. 9. According to the geological exploration results, the main geology excavated by the TBM is composed of gravelly sand, silty clay, medium-coarse sand and fully weathered granite, with bedrock bulges in some sections, and the bulging bedrock is moderately weathered granite with a saturated uniaxial compressive strength ranging from 35.4 to 138 MPa.

The project adopts the slurry TBM shown in Fig. 9, designed and manufactured by China Railway Engineering Equipment Group Co., Ltd. (CREG), with an excavation diameter of 15010 mm, a designed slurry chamber pressure of 6 bar, an opening cutterhead ratio of 28.5%, a total thrust force of 222200 kN, and 82 disc cutters. More detailed performance parameters are shown in Table 1.

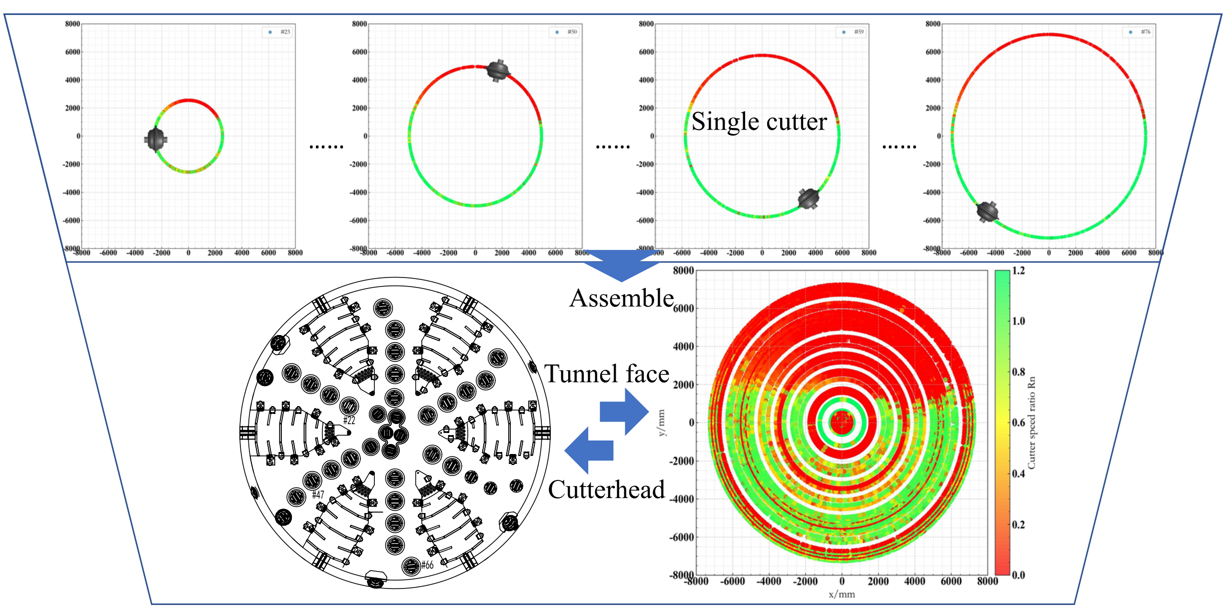

Fig. 8 The process of identifying the full-face tunnel face geological conditions

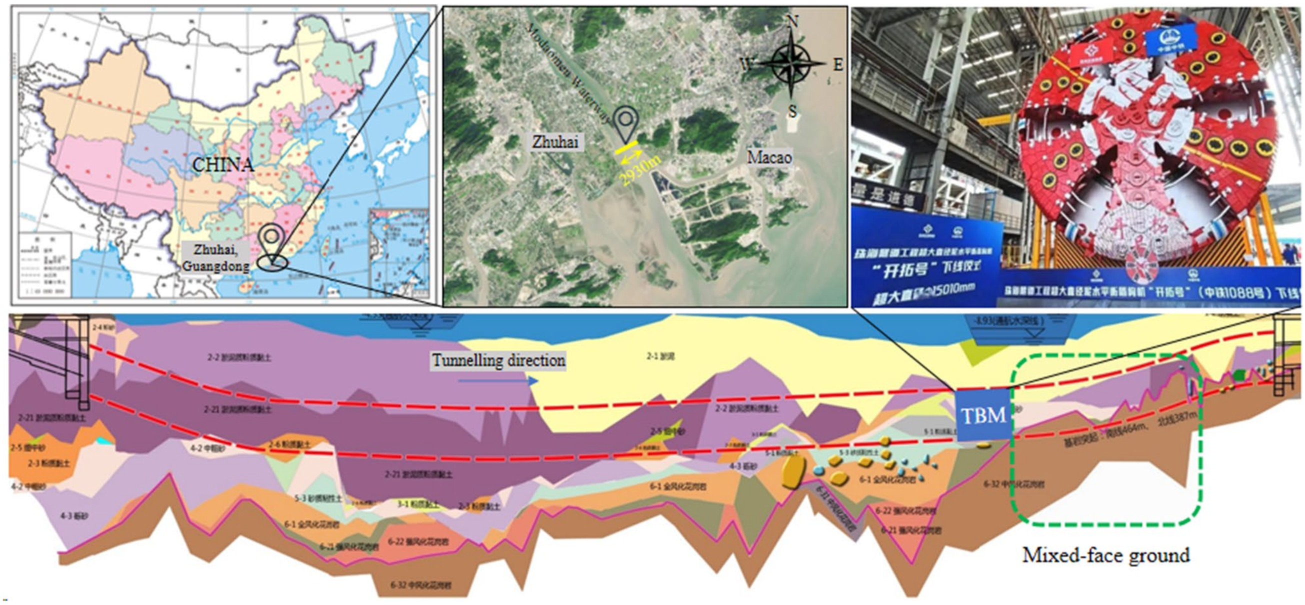

Fig. 9 Schematic of the project

Table 1 Main parameters of the slurry TBM

Parameter	Value	Unit	Parameter	Value	Unit
TBM type	Slurry TBM	/	Excavation diameter	15010	mm
Max. thrust speed	50	mm/min	Opening ratio	28.5	%
Max. thrust force	222200	kN	Qty. of disc cutters	82	pcs
Rated rotation speed	1.4	r/min	Qty. of scrapers	96	pcs
Rated torque	26707	kNm	Designed slurry chamber pressure	6	bar

The main parameters of the disc cutter working status include the rotation speed, load, and wear. From the analysis above, combined with the rock breaking mechanism by the disc cutter referred to in Section "Forces acting on the disc cutter during rock breaking" and the conditions for the disc cutter rotation, the disc cutter rotation speed ratio can reflect the difference in soft and hard layers, and monitoring of the rotation speed of the distributed disc cutter at the cutterhead can be used to identify mixed-face ground.

Wei et al. designed an electromagnetic rotation speed monitoring sensor (Wei et al. 2021), as shown in Fig. 10. Multiple magnets are embedded in the cutter ring of the disc cutter, and the rotation sensing devices are designed in the sensor probes on both sides. When the disc cutter rotates, the periodic pulse signal triggered by the magnetic field is used to judge and monitor the rotation of the disc cutter, and the real-time rotation speed of the disc cutter n_k in Fig. 8 is calculated by measuring the pulse period in Fig. 10.

The disc cutter rotation speed monitoring system made by the CREG has realized industrialized applications under complex construction conditions and stable signal transmission under multimedia conditions, and it has been applied on an EPB TBM, slurry TBM, hard rock TBM and other types of TBMs (Dujuan et al. 2021; Shunhui et al. 2020; Lianhui et al. 2023). Its reliability has been verified by multiple projects.

Characteristics of the disc cutter rotation speed in mixed-face ground

The borehole geological exploration results are shown in Fig. 10, and the geological conditions from ring 1222 to ring 1235 are mixed-face ground. This geological section comprises silty clay, medium-coarse sand and moderately weathered granite. During work in these rings, the workers are extremely cautious in TBM tunneling to avoid problems such as attitude deviation or tunnel collapse; the disc cutter working status monitoring system is well maintained, so the collected fusion data including tunneling parameters and working status monitoring data are of high quality. Consequently, we select the data of rings 1222 to 1235 to verify our proposed method. Moreover, we selected the data of ring 1522 to illustrate the data characteristics of the disc cutter in the full-face silty clay layer, which was used to prove the effectiveness of the method.

To analyze the characteristics of the disc cutter rotational speed, three sets of data are selected to calculate the speed ratio, namely, the data of the inner and the outer disc cutter of ring 1222 with mixed-face ground, as well as the data of

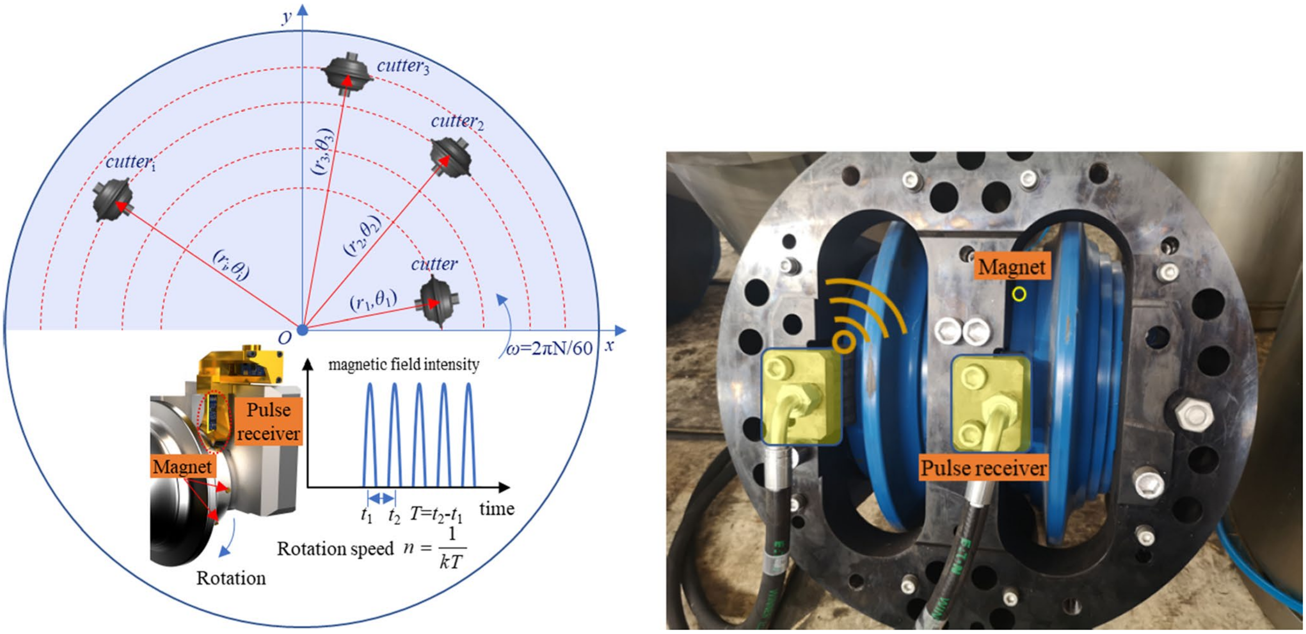

(a) method (b) entity

Fig. 10 Rotation speed monitoring method for distributed cutters

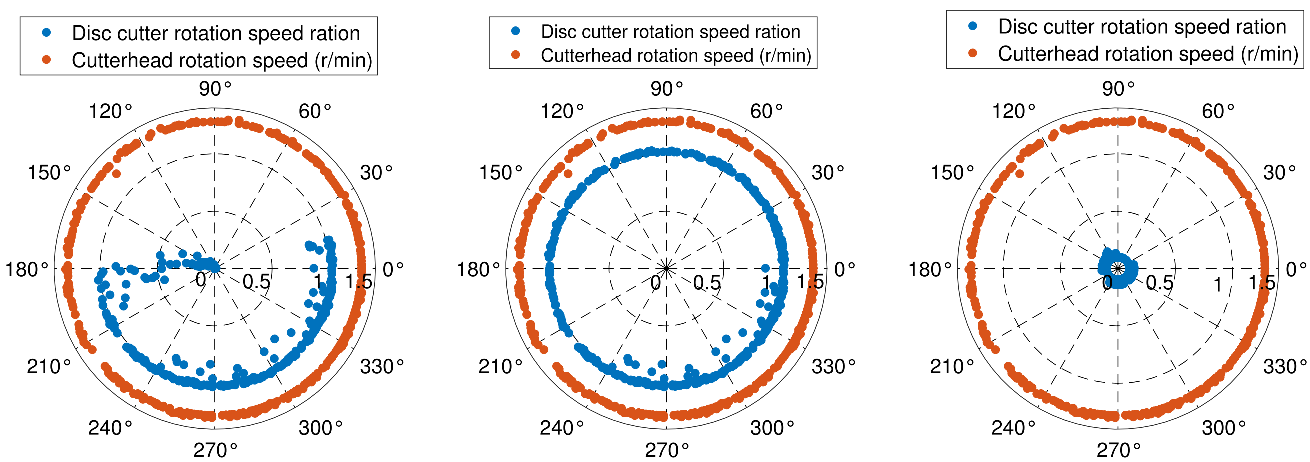

(a) 70# in ring 1222 (b) 7# in ring 1222 (c) 70# in ring 1522

Fig. 11 Disc cutter rotation speed ratio in mixed-face ground

the outer disc cutter of ring 1522 in the silty clay. The inner disc cutter number is 7, and the outer disc cutter number is 70.

Disc cutter rotation speed ratios of 7# and 70# during tunneling in the mixed face ground ring 1222 and that of 70# during tunneling in the silt layer ring 1522 are shown in Fig. 11. In ring 1222, the cutterhead rotation speed is 1.3 r/min, and the calculated disc cutter rotation speed ratio is distributed between 0 and 1.05 for the disc cutter 70#, as shown in Fig. 11(a). In the part between 15–170 °, the rotation speed ratio is close to 0; in the part between 170–180 °, the rotation speed ratio gradually increases from 0 to 1; then, the rotation speed ratio remains stable and fluctuates near 1 with the change in the disc cutter angle. In Fig. 11(b), the speed ratio is always 1 for the disc cutter 7#, which is located in the center area of the cutterhead. In Fig. 11(c), the speed ratio is always 0 for disc cutter 70# in ring 1522.

We can infer the ground through the data characteristics shown in these two graphs. For the arc area traveled by the disc cutter 70#, the ground is mainly soft soil between 15–170°, the ground is mainly hard rock between 180–360–15°, and the ground is the stratigraphic interface between 170–180°. For the arc area traveled by the disc cutter 7#, the ground is hard rock. For the arc area traveled by the disc cutter 70# in ring 1522, the ground is soft soil.

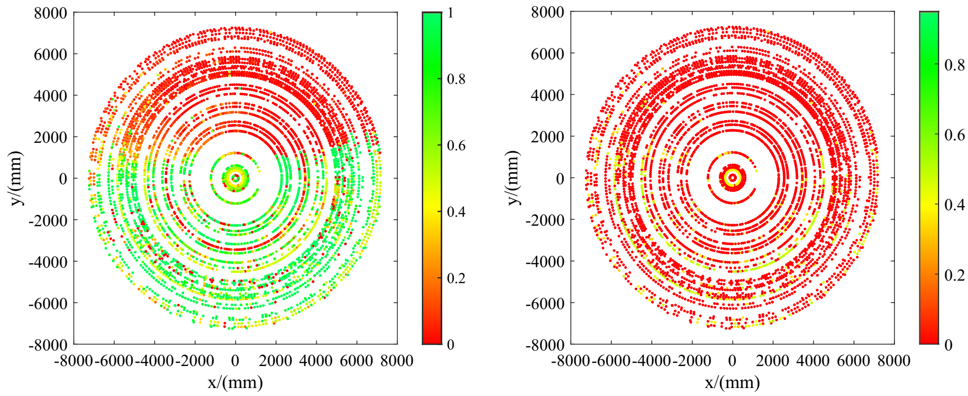

(a) Ring 1222 (b) Ring 1522

Fig. 12 Full-face disc cutter rotation speed ratio distribution

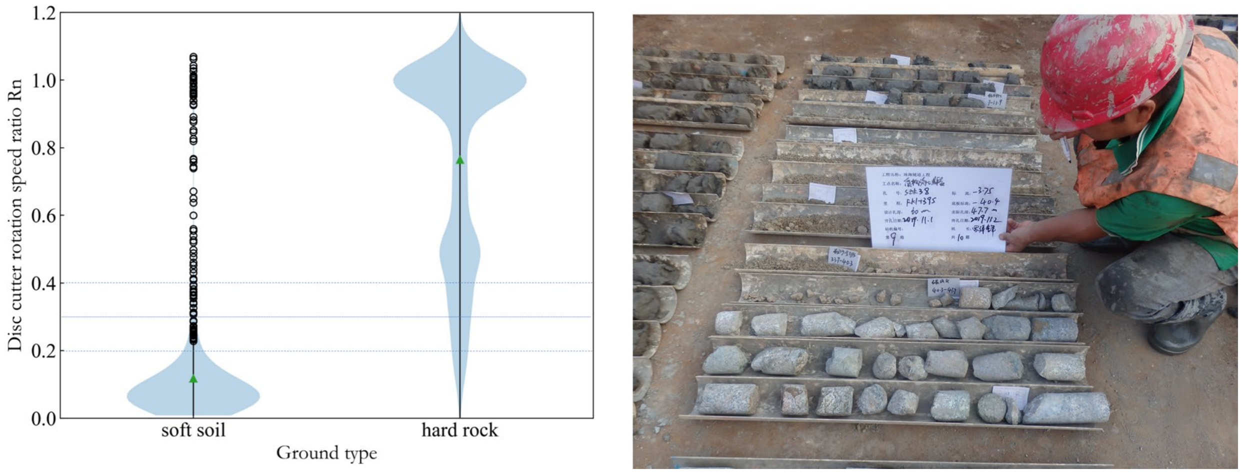

(a) Violin distribution of disc cutter rotation speed ratio (b) Drilling physical picture

Fig. 13 Comparison between the rotational speed distribution and the drilling data for ring 1222

Therefore, the rotation speed ratio is considerably different in mixed-face ground, so it is used to diagnose mixed-face ground; it can eliminate the influence of the installation radius, while the rotation speed abnormality characteristic can still be retained. The rotation speed ratio also considerably differs between soft soil and hard rock.

Determination of the precise diagnostic criteria for geology

Using the data of multiple disc cutters on the cutterhead, the full-face disc cutter rotation speed and disc cutter rotation speed ratio characteristics in rings 1222 and 1522 are obtained, as shown in Fig. 12. As seen from this figure, substantial differences exist in the distribution of the disc cutter rotation speed ratio among different rings and between different areas within the same ring.

To diagnose the mixed ground precisely, we should compute the threshold value of the rotation speed ratios between the hard and soft strata. We compared geological conditions within the range of the tunnel face with actual drill hole data and the results of the proposed method, and we obtained the distribution of the speed ratio R_n in the soft soil and hard rock layer as shown in Fig. 13(a). The core drilling process is shown in Fig. 13(b). In the soft layer, the speed ratio R_n is relatively small, mainly distributed within the range of $0 - 0.2$, indicating that the actual speed of the disc cutter is much lower than the theoretical speed and the disc cutter cannot rotate normally. In contrast, in the hard rock layer, the overall value of R_n is relatively large, usually greater than 0.4. Under relatively intact hard rock geological conditions, R_n is essentially distributed above 0.8, indicating that the disc cutter can rotate normally in the layer, and the actual speed is close to the theoretical speed. We have also verified that setting the threshold value as 0.2 or 0.4 makes little difference in the results compared with setting it as 0.3. Thus, we choose the threshold 0.3 as a compromise. Namely, $R_n = 0.3$ is a reasonable threshold for distinguishing between soft soil and hard rock. R_n is less than 0.3 in the soft soil layer but greater than 0.3 in the hard rock layer. This method can effectively distinguish between soft soil layers and hard rock layers.

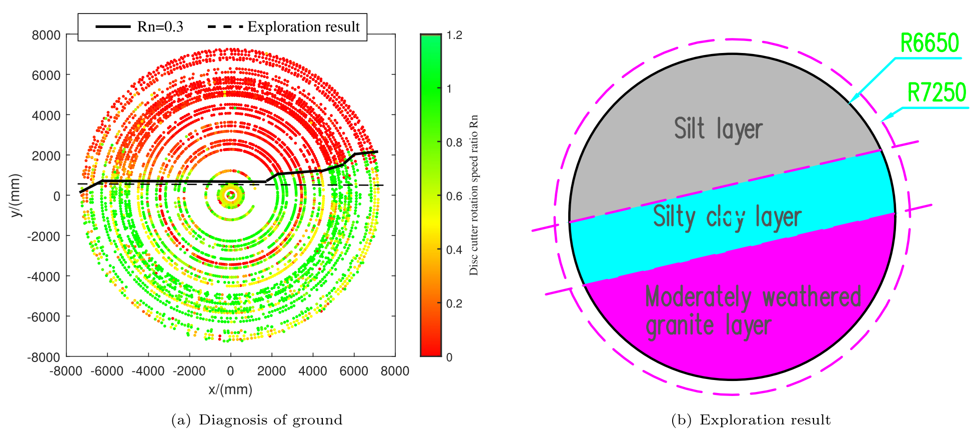

Fig. 14 Diagnosis of ground in ring 1222

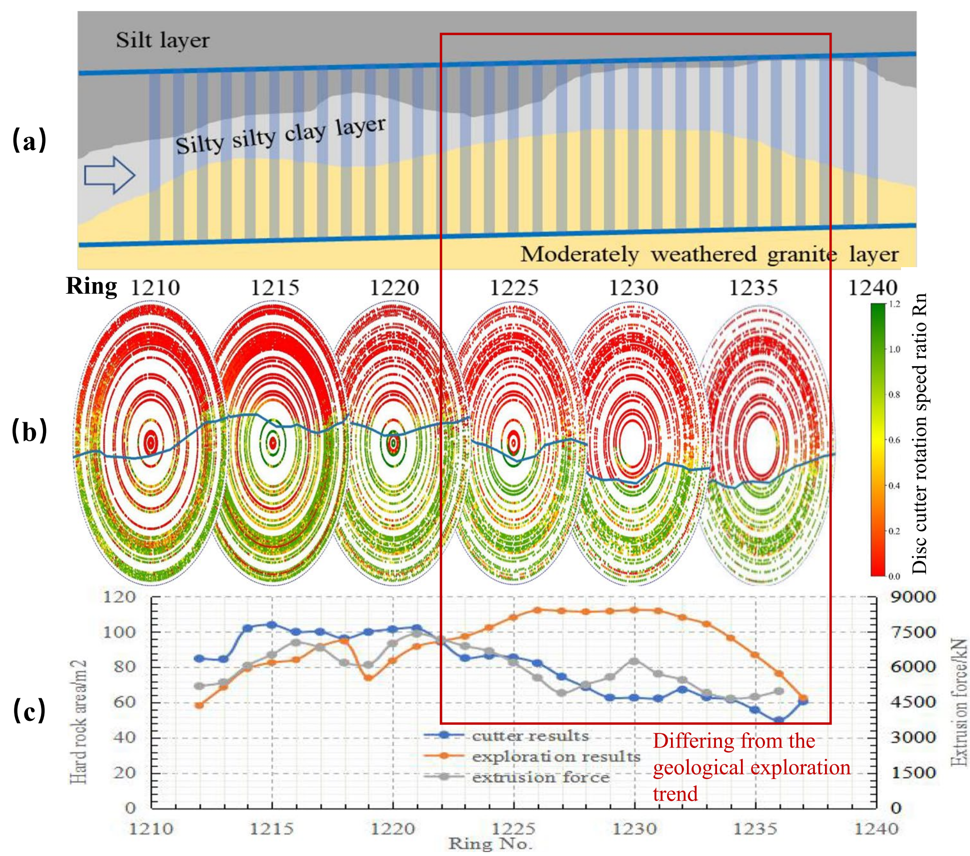

Fig. 15 Cross-validation of mixed-face ground diagnosis. (**a**) geological exploration; (**b**) proposed method; (**c**) tunneling parameters

An exploration report of ring 1222, which was obtained from the drilling data, is shown in Fig. 14(b) .

Three kinds of ground are found in ring 1222, namely, silt and silty clay and moderately weathered granite from top to bottom, respectively. By using the characteristics of the rotation speed ratio in different kinds of ground, the area of soft soil and hard rock ground on the tunnel face in ring 1222 can be obtained, as shown in Fig. 14(a).

The area of hard rock in this ring is calculated to be 94 m^2, accounting for 53% of the tunnel face, while the area of soft soil is 83 m^2, accounting for 47% of the tunnel face. A comparison with the exploration results shows that the proposed method is consistent with the findings reported in Fig. 14(b).

Discussion

By using the tunnel face results analyzed from the disc cutter working status data of multiple rings in this scope, we can obtain the mixed-face ground in this region of the excavated sections, as shown in Fig. 15(b).

The geological exploration results within this region are shown in Fig. 15(a). These results are typically obtained directly from borehole data. However, owing to constraints such as cost limitations and surface buildings, the borehole positions are often discontinuous. In this project, Zhuhai Tunnel, the borehole spacing is approximately 50 m, and the geological conditions between adjacent boreholes are inferred on the basis of data from neighboring boreholes. Consequently, the exploration results are accurate in regions where the borehole data are available, whereas potential errors may exist in other areas.

Compared with the exploration result, the geological conditions obtained using the proposed method are continuous. These two sets of results are compared in Fig. 15(a) and (b), which reveals that the rock face and the rock area have different heights. The largest hard rock area in the exploration results is 91.6 m^2 and 112.3 m^2 in rings 1221 and 1230, respectively, but the area diagnosed through cutter rotation speed ratios is 102 m^2 and 62.6 m^2. Moreover, widespread differences exist in the hard rock areas in rings 1222 to 1237.

To further confirm the actual geological conditions, we introduced the extrusion force of the cutterhead to conduct further analysis of the types of ground, using the method proposed by kos Tóth et al. (2013). The cutterhead extrusion force in this region was analyzed in conjunction with the two previous results, as illustrated in Fig. 15(c). The orange and blue curves represent the hard rock areas calculated from the geological exploration and the proposed method, respectively. The gray curve represents the cutterhead extrusion force. The extrusion force shows the same trend as that in the hard rock areas diagnosed by the disc cutter rotation speed ratio in rings 1222 to 1235; the extrusion force gradually decreases with decreasing hard rock area, whereas the geological exploration areas first increase but then decrease, which is uncoordinated with the extrusion force. The above analysis demonstrates the effectiveness of the proposed method.

Conclusions

This paper proposes a method for the precise and continuous diagnosis of mixed-face ground. This method does not rely on measuring the forces exerted on the disc cutter, thus reducing the adverse effects of vibrations and enhancing the practical applicability. The primary conclusions drawn from its application in the Zhuhai slurry TBM tunnel project are as follows:

(1) The tunnel face can be precisely characterized by the distributed disc cutter rotation status monitoring data. The disc cutter rotation speed ratio is a normalized parameter that integrates the disc cutter rotation speed, cutterhead rotation speed, disc cutter installation radius and disc cutter radius, which can eliminate the influence of the disc cutter installation parameters and tunneling parameters;

(2) The rotation speed ratio substantially differs for mixed-face ground. The disc cutters can rotate normally when the rotation speed ratio in hard rock areas is high, but they rotate abnormally when the soft soil area is small . The rotation speed ratio can be set to 0.3 to distinguish hard rock areas and soft rock areas;

(3) The proposed method can provide continuous geological diagnostic results and

can further correct geological exploration data.

Funding This work was supported by the National Key R&D Program of China (Intelligent construction technology for ultralong submarine tunnels, 2023YFB2603600).

References

Dujuan W, Weiwei Z, Jianian Z et al (2021) A device for measuring rotation speed and temperature of disc cutter of accessible cutter head and a method for measuring wear loss of disc cutter. Cn108181484b edn

Entacher M, Winter G, Galler R (2013) Cutter force measurement on tunnel boring machines - implementation at koralm tunnel. Tunn Underground Space Technol Incorpor Trenchless Technol Res 38(sep.):487–496

Entacher M, Winter G, Bumberger T et al (2012) Cutter force measurement on tunnel boring machines - system design. Tunn Underground Space Technol Incorporat Trenchless Technol Res 31(Complete):97–106

Farrokh E (2021) Cutter change time and cutter consumption for rock tbms. Tunn Undergr Space Technol 114(12):104000

Feng DJamal Li (2019) Modeling hard rock failure induced by structural planes around deep circular tunnels. Eng Fract Mech 205

Gong Q, Zhou X, Liu Y et al (2020) Development of a real-time muck analysis system for assistant intelligence tbm tunnelling. Tunn Underground Space Technol 107

Imv A, Cs B (2017) Prediction of tbm performance in mixed-face ground conditions. Tunn Undergr Space Technol 69:116–124

G.-J. L, T.-H. K (2023) Discharge behavior of spherical and rock chip mucks by screw conveyors in tbm: Physical model experiments and dem simulations. Tunn Underground Space Technol 142(Dec.):1.1-1.12

kos Tóth, Gong Q, Zhao J (2013) Case studies of tbm tunneling performance in rock-soil interface mixed ground. Tunn Undergr Space Technol 38:140–150

Li JB, Chen ZY, Li X et al (2023) Feedback on a shared big dataset for intelligent tbm part:feature extraction and machine learning methods. Underground Space

Li C, Hou S, Liu Y et al (2020) Analysis on the crown convergence deformation of surrounding rock for double-shield tbm tunnel based on advance borehole monitoring and inversion analysis. Tunn Undergr Space Technol 103:103513

Lianhui J, Zhiguo Z, Yongguang Z et al (2023) A monitoring system for TBM disc cutter wear. Cn115900540a edn

Li S, Liu B, Xu X et al (2017) An overview of ahead geological prospecting in tunneling. Tunn Underground Space Technol 63(MAR.):69–94

Ma, Hongsu, Yin, et al. (2015) Tbm tunneling in mixed-face ground: Problems and solutions. Int J Min Sci Technol 000(004):P.641-647

Qi W, Wang L, Zhou S et al (2021) Total loads modeling and geological adaptability analysis for mixed soil-rock tunnel boring machines. Underground Space

Rostami J, Ozdemir L, Nilson B (1996) Comparison between csm and nth hard rock tbm performance prediction models. In: Proceedings of annual technical meeting of the institute of shaft drilling technology, Las Vegas

Shunhui T, Xiaolong W, Fulong L et al (2020) A real-time monitoring system and method for TBM disc cutter load. China Patent Cn111236956a edn

Wang S, Wang Y, Li X et al (2021) Big data-based boring indexes and their application during tbm tunneling. Hindawi Limited

Wei X, Lin F, Meng X et al (2021) Real-time diagnosis application of disc cutter in super-large diameter slurry shield: a case study on shantou suai tunnel. Tunn Construct 41(05):865–870

Xie WQ, Zhang XP, Liu XL et al (2023) Real-time perception of rock-machine interaction information in tbm tunnelling using muck image analysis. Tunn Underground Space Technol

Zhang Y, Liu Z, Bai P et al (2023) Multi-borehole three-dimensional induced polarization tomography method for tunnel water hazards ahead prospecting. Tunn Underground Space Technol 133:104952